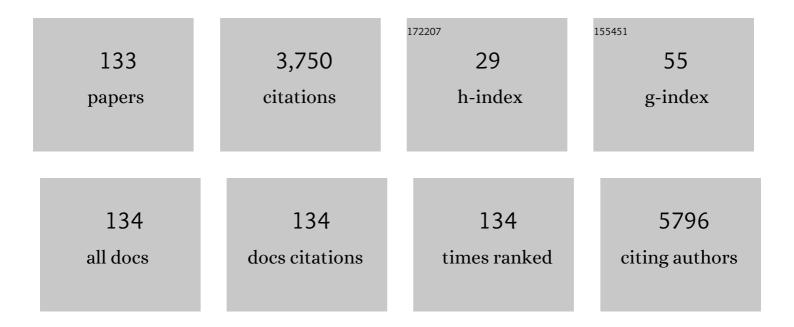
Miodrag N Mitrić

List of Publications by Year in descending order

Source: https://exaly.com/author-pdf/3214096/publications.pdf Version: 2024-02-01



ΜΙΟΠΡΛΟ Ν ΜΙΤΡΙÄT

#	Article	IF	CITATIONS
1	Synthesis, characterization and antimicrobial activity of copper and zinc-doped hydroxyapatite nanopowders. Applied Surface Science, 2010, 256, 6083-6089.	3.1	461
2	Synthesis of antimicrobial monophase silver-doped hydroxyapatite nanopowders for bone tissue engineering. Applied Surface Science, 2011, 257, 4510-4518.	3.1	221
3	Bioactive hydroxyapatite/graphene composite coating and its corrosion stability in simulated body fluid. Journal of Alloys and Compounds, 2015, 624, 148-157.	2.8	167
4	Nanomaterial with High Antimicrobial Efficacy—Copper/Polyaniline Nanocomposite. ACS Applied Materials & Interfaces, 2015, 7, 1955-1966.	4.0	140
5	Interfacial Synthesis of Gold–Polyaniline Nanocomposite and Its Electrocatalytic Application. ACS Applied Materials & Interfaces, 2015, 7, 28393-28403.	4.0	122
6	Multisite luminescence of rare earth doped TiO2 anatase nanoparticles. Materials Chemistry and Physics, 2012, 135, 1064-1069.	2.0	117
7	Synthesis and characterization of monetite and hydroxyapatite whiskers obtained by a hydrothermal method. Ceramics International, 2011, 37, 167-173.	2.3	116
8	Electrocatalysis of oxygen reduction reaction on polyaniline-derived nitrogen-doped carbon nanoparticle surfaces in alkaline media. Journal of Power Sources, 2012, 220, 306-316.	4.0	105
9	Corrosion Stability and Bioactivity in Simulated Body Fluid of Silver/Hydroxyapatite and Silver/Hydroxyapatite/Lignin Coatings on Titanium Obtained by Electrophoretic Deposition. Journal of Physical Chemistry B, 2013, 117, 1633-1643.	1.2	95
10	Arsenate adsorption on waste eggshell modified by goethite, α-MnO2 and goethite/α-MnO2. Chemical Engineering Journal, 2014, 237, 430-442.	6.6	75
11	Preparation of Y2O3:Eu3+ nanopowders via polymer complex solution method and luminescence properties of the sintered ceramics. Ceramics International, 2011, 37, 525-531.	2.3	67
12	High-rate intercalation capability of NaTi2(PO4)3/C composite in aqueous lithium and sodium nitrate solutions. Journal of Power Sources, 2015, 288, 176-186.	4.0	62
13	Superior photocatalytic properties of carbonized PANI/TiO2 nanocomposites. Applied Catalysis B: Environmental, 2017, 213, 155-166.	10.8	62
14	Mineralized agar-based nanocomposite films: Potential food packaging materials with antimicrobial properties. Carbohydrate Polymers, 2017, 175, 55-62.	5.1	59
15	The effect of graphene loading on mechanical, thermal and biological properties of poly(vinyl) Tj ETQq1 1 0.7843	14 rgBT /0 2.9	Dverlock 10 T
16	Microporous conducting carbonized polyaniline nanorods: Synthesis, characterization and electrocatalytic properties. Microporous and Mesoporous Materials, 2012, 152, 50-57.	2.2	52
17	Electrochemical behaviour of V2O5 xerogel in aqueous LiNO3 solution. Electrochemistry Communications, 2009, 11, 1512-1514.	2.3	50
18	Highly Active Rutile TiO ₂ Nanocrystalline Photocatalysts. ACS Applied Materials & Interfaces, 2020, 12, 33058-33068.	4.0	46

#	Article	IF	CITATIONS
19	Synthesis of metastable hard-magnetic ε-Fe ₂ O ₃ nanoparticles from silica-coated akaganeite nanorods. Nanoscale, 2017, 9, 10579-10584.	2.8	45
20	Study of chitosan/xanthan gum polyelectrolyte complexes formation, solid state and influence on ibuprofen release kinetics. International Journal of Biological Macromolecules, 2020, 148, 942-955.	3.6	45
21	In situ synthesis of Cu/Cu2O nanoparticles on the TEMPO oxidized cotton fabrics. Cellulose, 2018, 25, 829-841.	2.4	42
22	Synthesis and antimicrobial properties of Zn-mineralized alginate nanocomposites. Carbohydrate Polymers, 2017, 165, 313-321.	5.1	41
23	Dissolution rate enhancement and physicochemical characterization of carbamazepine-poloxamer solid dispersions. Pharmaceutical Development and Technology, 2016, 21, 268-276.	1.1	40
24	Synthesis and characterization of LiFePO4/C composite obtained by sonochemical method. Solid State Ionics, 2008, 179, 415-419.	1.3	38
25	Ultrasonic assisted arsenate adsorption on solvothermally synthesized calcite modified by goethite, α-MnO2 and goethite/α-MnO2. Ultrasonics Sonochemistry, 2014, 21, 790-801.	3.8	37
26	Visible-light active mesoporous, nanocrystalline N,S-doped and co-doped titania photocatalysts synthesized by non-hydrolytic sol-gel route. Ceramics International, 2016, 42, 16718-16728.	2.3	35
27	Annealing effects on the microstructure and photoluminescence of Eu3+-doped GdVO4 powders. Optical Materials, 2013, 35, 1797-1804.	1.7	34
28	Level Set Approach to Anisotropic Wet Etching of Silicon. Sensors, 2010, 10, 4950-4967.	2.1	33
29	Preparation of LiFePO4/C composites by co-precipitation in molten stearic acid. Journal of Power Sources, 2011, 196, 4613-4618.	4.0	32
30	In situ photoreduction of Ag+-ions by TiO2 nanoparticles deposited on cotton and cotton/PET fabrics. Cellulose, 2014, 21, 3781-3795.	2.4	31
31	Structural and electrical properties of the 2Bi2O3·3ZrO2 system. Journal of Solid State Chemistry, 2008, 181, 1321-1329.	1.4	29
32	Functionalization of carbon nanotubes with silver clusters. Applied Surface Science, 2010, 256, 7048-7055.	3.1	29
33	Highâ€efficiency Sb ₂ S ₃ â€based hybrid solar cell at low light intensity: cell made of synthesized Cu and Seâ€doped Sb ₂ S ₃ . Progress in Photovoltaics: Research and Applications, 2016, 24, 704-715.	4.4	29
34	Nonconvex Hamiltonians in three dimensional level set simulations of the wet etching of silicon. Applied Physics Letters, 2006, 89, 213102.	1.5	28
35	Cyclic voltammetry of LiCr0.15Mn1.85O4 in an aqueous LiNO3 solution. Journal of Power Sources, 2007, 174, 1117-1120.	4.0	28
36	The effect of Sn for Ti substitution on the average and local crystal structure of BaTi _{1â^'} <i>_x</i> Sn <i>_x</i> O ₃ (0 ≤i>x≤0.20). Journal of Applied Crystallography, 2014, 47, 999-1007.	1.9	28

#	Article	IF	CITATIONS
37	The effect of lignin on the structure and characteristics of composite coatings electrodeposited on titanium. Progress in Organic Coatings, 2012, 75, 275-283.	1.9	26
38	Anisotropic silver nanoparticles as filler for the formation of hybrid nanocomposites. Materials Research Bulletin, 2013, 48, 52-57.	2.7	26
39	The influence of triangular silver nanoplates on antimicrobial activity and color of cotton fabrics pretreated with chitosan. Journal of Materials Science, 2014, 49, 4453-4460.	1.7	26
40	Ferromagnetic polyaniline/TiO ₂ nanocomposites. Polymer Composites, 2012, 33, 1482-1493.	2.3	25
41	Hydrothermal synthesis of Li4Ti5O12/C nanostructured composites: Morphology and electrochemical performance. Materials Research Bulletin, 2013, 48, 218-223.	2.7	24
42	Structural and magnetic properties of hydrothermally synthesized β-MnO2 and α-K MnO2 nanorods. Journal of Alloys and Compounds, 2016, 665, 261-270.	2.8	24
43	The LiFe(1â^')V PO4/C composite synthesized by gel-combustion method, with improved rate capability and cycle life in aerated aqueous solutions. Electrochimica Acta, 2013, 109, 835-842.	2.6	23
44	Thermal, morphological, and mechanical properties of ethyl vanillin immobilized in polyvinyl alcohol by electrospinning process. Journal of Thermal Analysis and Calorimetry, 2014, 118, 661-668.	2.0	23
45	Structural, spectroscopic and crystal field analyses of Ni2+ andÂCo2+ doped Zn2SiO4 powders. Applied Physics A: Materials Science and Processing, 2011, 104, 483-492.	1.1	22
46	Influence of different pore-forming agents on wollastonite microstructures and adsorption capacities. Ceramics International, 2017, 43, 7461-7468.	2.3	21
47	The thermal stability of porous alumina/stainless steel catalyst support obtained by spray pyrolysis. Applied Surface Science, 2008, 255, 3049-3055.	3.1	20
48	Preparation of TiO2/carbon nanotubes photocatalysts: The influence of the method of oxidation of the carbon nanotubes on the photocatalytic activity of the nanocomposites. Ceramics International, 2012, 38, 6123-6129.	2.3	20
49	Characterization of poly(vinyl alcohol)/gold nanocomposites obtained by <i>in situ</i> gammaâ€irradiation method. Journal of Applied Polymer Science, 2012, 125, 1244-1251.	1.3	20
50	Luminescence thermometry via the two-dopant intensity ratio of Y2O3:Er3+, Eu3+. Journal Physics D: Applied Physics, 2016, 49, 485104.	1.3	19
51	Optical, structural and thermal characterization of gold nanoparticles – poly(vinylalcohol) composite films. Journal of Composite Materials, 2012, 46, 987-995.	1.2	18
52	Vibrational and electron paramagnetic resonance spectroscopic studies of Î ² -MnO2 and α-K MnO2 nanorods. Journal of Alloys and Compounds, 2017, 728, 259-270.	2.8	18
53	The influence of fluorine doping on the structural and electrical properties of the LiFePO4 powder. Ceramics International, 2017, 43, 3224-3230.	2.3	18
54	The influence of coating with aminopropyl triethoxysilane and CuO/Cu 2 O nanoparticles on antimicrobial activity of cotton fabrics under dark conditions. Journal of Applied Polymer Science, 2020, 137, 49194.	1.3	18

#	Article	IF	CITATIONS
55	Oxygen reduction reaction of Pt–In alloy: Combined theoretical and experimental investigations. Electrochimica Acta, 2013, 114, 706-712.	2.6	17
56	New insights into BaTi _{1–<i>x</i>} Sn _{<i>x</i>} O ₃ (0 ≤i>x â% 1726-1733.	₀)¤Tj ETQq0 1.9	0 0 rgBT /Ove 17
57	Bimetallic alginate nanocomposites: New antimicrobial biomaterials for biomedical application. Materials Letters, 2018, 212, 32-36.	1.3	17
58	One-pot synthesis of novel silver-polyaniline-polyvinylpyrrolidone electrocatalysts for efficient oxygen reduction reaction. Electrochimica Acta, 2018, 281, 549-561.	2.6	17
59	The effect of the addition of colloidal iridium oxide into sol–gel obtained titanium and ruthenium oxide coatings on titanium on their electrochemical properties. Physical Chemistry Chemical Physics, 2010, 12, 7521.	1.3	16
60	Natural sorbents modified by divalent Cu2+- and Zn2+- ions and their corresponding antimicrobial activity. New Biotechnology, 2017, 39, 150-159.	2.4	16
61	Ligand mediated synthesis of AgInSe2 nanoparticles with tetragonal/orthorhombic crystal phases. Journal of Nanoparticle Research, 2012, 14, 1.	0.8	15
62	Influence of MgO addition on the synthesis and electrical properties of sintered zinc–titanate ceramics. Journal of Alloys and Compounds, 2009, 471, 272-277.	2.8	14
63	Kinetics of hydrogen absorption in Zr-based alloys. Journal of Alloys and Compounds, 2013, 559, 162-166.	2.8	14
64	The use of various dicarboxylic acids as a carbon source for the preparation of LiFePO4/C composite. Ceramics International, 2015, 41, 6753-6758.	2.3	14
65	Structural, Optical, and Electrical Properties of Applied Amorphized and Polycrystalline Sb2S3 Thin Films. Metallurgical and Materials Transactions A: Physical Metallurgy and Materials Science, 2016, 47, 1460-1468.	1.1	14
66	Effects of fluorination on the structure, magnetic and electrochemical properties of the P2-type NaxCoO2 powder. Journal of Alloys and Compounds, 2019, 774, 30-37.	2.8	14
67	Electrochemical properties of nanostructured Li1.2V3O8 in aqueous LiNO3 solution. Electrochimica Acta, 2011, 56, 6469-6473.	2.6	13
68	In situ photoreduction of Ag+-ions on the surface of titania nanotubes deposited on cotton and cotton/PET fabrics. Cellulose, 2017, 24, 1597-1610.	2.4	13
69	Electrochemical tuning of capacitive response of graphene oxide. Physical Chemistry Chemical Physics, 2018, 20, 22698-22709.	1.3	13
70	Colloidal synthesis of Sb2S3 nanorods/bars with strong preferred orientation. Materials Letters, 2011, 65, 1919-1922.	1.3	12
71	Synthesis and Properties of a New Dental Material Based on Nano‣tructured Highly Active Calcium Silicates and Calcium Carbonates. International Journal of Applied Ceramic Technology, 2014, 11, 57-64.	1.1	12
72	The porosity and roughness of electrodeposited calcium phosphate coatings in simulated body fluid. Journal of the Serbian Chemical Society, 2015, 80, 237-251.	0.4	12

Miodrag N Mitrić

#	Article	IF	CITATIONS
73	Formation of ZnIn2S4 nanosheets and tubular structures in organic media. Materials Research Bulletin, 2017, 87, 140-147.	2.7	12
74	Gamma irradiation induced in situ synthesis of lead sulfide nanoparticles in poly(vinyl alcohol) hydrogel. Radiation Physics and Chemistry, 2017, 130, 282-290.	1.4	12
75	Efficient and novel Sb ₂ S ₃ based solar cells with chitosan/poly(ethylene) Tj ETQq1 1 ().784314 r 2.2	gBT /Overlock
76	Isotopeâ€like effect in YVO ₄ :Eu ³⁺ nanopowders: Raman spectroscopy. Journal of Raman Spectroscopy, 2019, 50, 802-808.	1.2	12
77	Broad Spectrum of Antimicrobial Activity of Cotton Fabric Modified with Oxalic Acid and CuO/Cu2O Nanoparticles. Fibers and Polymers, 2019, 20, 2317-2325.	1.1	12
78	Structural characteristics and bonding environment of Ag nanoparticles synthesized by gamma irradiation within thermoâ€responsive poly(<scp><i>N</i></scp> â€isopropylacrylamide) hydrogel. Polymer Composites, 2017, 38, 1014-1026.	2.3	11
79	Insertion of lithium ion in anatase TiO 2 nanotube arrays of different morphology. Journal of Alloys and Compounds, 2017, 712, 90-96.	2.8	11
80	Growth and quantum confinement in Agl nanowires. Materials Letters, 2007, 61, 3522-3525.	1.3	10
81	Growth of Sb2S3 nanowires synthesized by colloidal process and self-assembly of amorphous spherical Sb2S3 nanoparticles in wires formation. Metals and Materials International, 2012, 18, 989-995.	1.8	10
82	Microstructural Analysis and the Multicolor UV/Violet/Blue/Green/Yellow PL Observed from the Synthesized ZnO Nano-leaves and Nano-rods. Metallurgical and Materials Transactions A: Physical Metallurgy and Materials Science, 2015, 46, 3679-3686.	1.1	10
83	Characterization and current–voltage characteristics of solar cells based on the composite of synthesized Sb ₂ S ₃ powder with small band gap and natural dye. Environmental Progress and Sustainable Energy, 2016, 35, 512-516.	1.3	10
84	Structural properties of the multiwall carbon nanotubes/poly(methyl methacrylate) nanocomposites: Effect of the multiwall carbon nanotubes covalent functionalization. Polymer Composites, 2017, 38, E472.	2.3	10
85	The role of low light intensity: A cheap, stable, and solidly efficient amorphous Sb ₂ S ₃ powder/hypericin composite/PVA matrix loaded with electrolyte solar cell. Environmental Progress and Sustainable Energy, 2017, 36, 1507-1516.	1.3	10
86	The synthesis of single phase WC nanoparticles/C composite by solid state reaction involving nitrogen-rich carbonized polyaniline. Ceramics International, 2013, 39, 8761-8765.	2.3	9
87	The effect of different extractants on lead desorption from a natural mineral. Applied Surface Science, 2015, 324, 221-231.	3.1	9
88	Weak Light Performance of Synthesized Amorphous <inline-formula> <tex-math>\${m Sb}_{2}{m S}_{3}\$ </tex-math> </inline-formula> -Based Hybrid Solar Cell. IEEE Journal of Photovoltaics, 2016, 6, 473-479.	1.5	9
89	The role of low light intensity: A step towards understanding the connection between light, optic/lens and photovoltaic behavior for Sb2S3 thin-film solar cells. Optics and Laser Technology, 2018, 101, 425-432.	2.2	9
90	The improved photovoltaic response of commercial monocrystalline Si solar cell under natural and artificial light by using water flow lens (WFL) system. International Journal of Energy Research, 2019, 43, 3507-3515.	2.2	9

#	Article	IF	CITATIONS
91	Physico-chemical characteristics of gamma irradiation crosslinked poly(vinyl alcohol)/magnetite ferrogel composite. Hemijska Industrija, 2014, 68, 743-753.	0.3	9
92	Influence of ultrasonic processing on the macromolecular properties of poly (d,l-lactide-co-glycolide) alone and in its biocomposite with hydroxyapatite. Ultrasonics Sonochemistry, 2010, 17, 902-908.	3.8	8
93	Organic Synthesis with Different OA/EHA Ratios of Sb2S3 Nanowires of Flower-Like Organization and [010] Orientation. Metallurgical and Materials Transactions A: Physical Metallurgy and Materials Science, 2012, 43, 1405-1409.	1.1	8
94	Influence of sulphide precursor on crystal phase of ternary I–III–VI2 semiconductors. Journal of Nanoparticle Research, 2013, 15, 1.	0.8	8
95	Properties of quenched LiFePO4/C powder obtained via cellulose matrix-assisted method. Powder Technology, 2013, 246, 539-544.	2.1	8
96	Nanostructured Fe2O3/TiO2 thick films: Analysis of structural and electronic properties. Ceramics International, 2015, 41, 6889-6897.	2.3	8
97	The influence of synthesis conditions on the redox behaviour of LiFePO4 in aqueous solution. Journal of Alloys and Compounds, 2019, 776, 475-485.	2.8	8
98	High performance of solvothermally prepared VO2(B) as anode for aqueous rechargeable lithium batteries. Journal of the Serbian Chemical Society, 2015, 80, 685-694.	0.4	8
99	Structural and optical investigation of gadolinia-doped ceria powders prepared by polymer complex solution method. International Journal of Materials Research, 2012, 103, 884-888.	0.1	7
100	Colloidal-chemistry based synthesis of quantized CuInS2/Se2 nanoparticles. Journal of the Serbian Chemical Society, 2012, 77, 789-797.	0.4	7
101	Crystal structure studies on plate/shelf like disodium ditungstate. Bulletin of Materials Science, 2013, 36, 149-152.	0.8	7
102	Surface coverage determination of iron-phosphate coatings on steel using voltammetric anodic dissolution technique. Journal of the Serbian Chemical Society, 2013, 78, 101-114.	0.4	7
103	Electronic aspects of formation and properties of local structures around Mn in Cd 1â^'x Mn x Te 1â^'y Se y. Materials Chemistry and Physics, 2015, 167, 236-245.	2.0	7
104	Reaction kinetics of mechanically activated cordierite-based ceramics studied via DTA. Journal of Thermal Analysis and Calorimetry, 2016, 124, 667-673.	2.0	7
105	Tailoring the physico-chemical and antimicrobial properties of agar-based films by in situ formation of Cu-mineral phase. European Polymer Journal, 2019, 119, 352-358.	2.6	7
106	Structural and magnetic properties of mechanochemically synthesized nanocrystalline titanium monoxide. Hemijska Industrija, 2012, 66, 181-186.	0.3	7
107	Structure of Disodium Dimolybdate Synthesized Using Thermodynamically Stable Molybdenum (VI) Oxide Clusters as Precursors. Journal of the American Ceramic Society, 2009, 92, 2467-2470.	1.9	6
108	Rare-earth doped (Lu0.85Y0.15)2SiO5 nanocrystalline powders obtained by polymer assisted sol–gel synthesis. Radiation Measurements, 2010, 45, 475-477.	0.7	6

#	Article	IF	CITATIONS
109	Ultra-High and Near-Zero Refractive Indices of Magnetron Sputtered Thin-Film Metamaterials Based on Ti _{<i>x</i>} O _{<i>y</i>} . Advances in Materials Science and Engineering, 2016, 2016, 1-9.	1.0	6
110	Developing an advanced electrocatalyst derived from triangular silver nanoplates@polyvinylpyrrolidone-polyaniline nanocomposites. Synthetic Metals, 2019, 257, 116173.	2.1	6
111	A study of defect structures in Fe-alloyed ZnO: Morphology, magnetism, and hyperfine interactions. Journal of Applied Physics, 2019, 126, .	1.1	6
112	Novel organo-colloidal synthesis, optical properties, and structural analysis of antimony sesquioxide nanoparticles. Journal of Nanoparticle Research, 2013, 15, 1.	0.8	5
113	Viscoelastic properties of poly(ε aprolactone)/clay nanocomposites in solid and in melt state. Journal of Applied Polymer Science, 2016, 133, .	1.3	5
114	Microsized fayalite Fe2SiO4 as anode material: the structure, electrochemical properties and working mechanism. Journal of Electroceramics, 2021, 47, 31-41.	0.8	5
115	Sintering of fly ash based composites with zeolite and bentonite addition for application in construction materials. Science of Sintering, 2017, 49, 23-37.	0.5	5
116	Novel Lowâ€Temperature Synthesis of Disodium Dimolybdate by Ultrasonic Spray Pyrolysis. Journal of the American Ceramic Society, 2007, 90, 4030-4032.	1.9	4
117	Novel morphology of needle-Like nanoparticles of Na2Mo2O7 synthesized by using Ultrasonic spray pyrolysis. Materials Research, 2013, 16, 44-49.	0.6	4
118	Preparation and characterization of bismuth germanium oxide (BGO) polymer composites. Journal of Alloys and Compounds, 2017, 695, 841-849.	2.8	4
119	Structural and electrochemical properties of the Li2FeP2O7/C composite prepared using soluble methylcellulose. Journal of Alloys and Compounds, 2019, 786, 912-919.	2.8	4
120	NANOSTRUCTURED ZrO2 POWDER SYNTHESIZED BY ULTRASONIC SPRAY PYROLYSIS. Surface Review and Letters, 2007, 14, 915-919.	0.5	3
121	Structural and optical characterization of hemimorphite with flower-like morphology synthesized by a novel low-temperature method. Materials Letters, 2012, 85, 138-141.	1.3	3
122	The use of methylcellulose for the synthesis of Li2FeSiO4/C composites. Cellulose, 2016, 23, 239-246.	2.4	3
123	Magnetic memory effect in hollandite-type α-K MnO2 monocrystalline nanorods. Journal of Alloys and Compounds, 2020, 820, 153406.	2.8	3
124	Towards a green and cost-effective synthesis of polyanionic cathodes: comparative electrochemical behaviour of LiFePO4/C, Li2FeP2O7/C and Li2FeSiO4/C synthesized using methylcellulose matrix. Bulletin of Materials Science, 2021, 44, 1.	0.8	3
125	Study of the effect of Mg (II) addition and the annealing conditions on the structure of mesoporous aluminum oxide using Plackett-Burman design. Journal of the Serbian Chemical Society, 2015, 80, 1529-1540.	0.4	3
126	Ground-state magnetism of chromium-substituted LiMn2O4 spinel. Journal of Magnetism and Magnetic Materials, 2008, 320, 943-949.	1.0	2

#	Article	IF	CITATIONS
127	Electrochemical behavior of H3PW12O40/ acid-activated bentonite powders. Chemical Industry and Chemical Engineering Quarterly, 2012, 18, 329-338.	0.4	2
128	Radiolytic synthesis and characterization of PVA/Au nanocomposites: The influence of pH values. Hemijska Industrija, 2008, 62, 101-106.	0.3	2
129	Magnetic properties of nanostructured SiOo2:Eu3+ powders. Journal of the Serbian Chemical Society, 2006, 71, 413-420.	0.4	2
130	Magnetic properties of ErxY1â^'xF3 solid solutions. Solid State Communications, 2005, 133, 157-161.	0.9	1
131	Structural and magnetic properties of mechanochemically synthesized nanosized yttrium titanate. Hemijska Industrija, 2012, 66, 309-315.	0.3	1
132	Investigation of structural, microstructural and magnetic properties of Yb Y1-F3 solid solutions. Journal of Physics and Chemistry of Solids, 2020, 142, 109449.	1.9	0
133	Survey of Electronic and Local Structural Properties of Cd _{1â^'} <i>_x</i> Co <i>_x</i> Se _{1â^'} <i>_y</i> Te(S)< by XAFS. Journal of the Physical Society of Japan, 2022, 91, .	i> œ¤ b>y	